

Electron energy relaxation times from ballistic-electron-emission spectroscopy

K. Reuter

*Instituto de Ciencia de Materiales (CSIC), Cantoblanco, E-28049 Madrid, Spain
and Lehrstuhl für Festkörperphysik, Universität Erlangen-Nürnberg, D-91058 Erlangen, Germany*

U. Hohenester

Istituto Nazionale per la Fisica della Materia and Dipartimento de Fisica, Università de Modena, I-41100 Modena, Italy

P. L. de Andres

Instituto de Ciencia de Materiales (CSIC), Cantoblanco, E-28049 Madrid, Spain

F. J. García-Vidal and F. Flores

Departamento de Física Teórica de la Materia Condensada, Universidad Autónoma de Madrid, E-28049 Madrid, Spain

K. Heinz

Lehrstuhl für Festkörperphysik, Universität Erlangen-Nürnberg, D-91058 Erlangen, Germany

P. Kocevar

Institut für Theoretische Physik, Karl-Franzens-Universität Graz, A-8010 Graz, Austria

(Received 21 January 1999; revised manuscript received 25 October 1999)

Using a Green's-function approach that incorporates band-structure effects, and a complementary k -space Monte-Carlo analysis, we show how to get a theoretically consistent determination of the inelastic mean free path $\lambda_{ee}(E)$ due to electron-electron interaction from ballistic electron emission spectroscopy. Exploiting experimental data taken at $T=77$ K on a thin-Au film (<100 Å) deposited on a Si substrate, we find that the energy dependence of $\lambda_{ee}(E)$ predicted by the standard Fermi-liquid theory provides excellent agreement between theoretical and experimental $I(V)$ spectra. In agreement with theories for real metals, an enhancement of $\lambda_{ee}(E)$ by a factor of two with respect to its electron-gas value is found.

Despite their manifest importance for the optimization of future nanometer scale electronic devices, hot carrier lifetimes in metals at energies close to the Fermi energy ($E_F < E < E_F + 5$ eV) are far from being completely understood from a fundamental point of view. Surprisingly, a particularly large uncertainty concerning even the quoted absolute order of magnitude has to be admitted for the mean free path (MFP) $\lambda_{ee}(E)$ due to inelastic electron-electron (e-e) scattering.¹ This is the more surprising as e-e scattering constitutes the predominant contribution to the electron energy relaxation for approximately $E > E_F + 1$ eV. The commonly accepted theoretical description for these processes is based on general considerations for a Fermi liquid,² predicting in the neighborhood of E_F : $\lambda_{ee}(E) \propto (E - E_F)^{-2}$. Within the random phase approximation (RPA) Quinn³ has derived the following expression:

$$\lambda_{ee}(E) = \lambda_0^{RPA}(r_s) \frac{\frac{E}{E_F}}{\left(\frac{E}{E_F} - 1\right)^2}. \quad (1)$$

For a homogeneous electron gas, the proportionality constant can be computed by a simple interpolating polynomial depending only on the metal density: $\lambda_0^{RPA}(r_s) \approx 4(1 + r_s)$; with λ_0^{RPA} obtained in a.u. and $1 \leq r_s \leq 6$. Yet, it has been recognized that λ_0^{RPA} can be substantially affected by differ-

ent levels of sophistication in the model. The contribution to the dielectric function of d electrons⁴ and electron exchange corrections,⁵ as well as the effect of flattened Fermi surfaces and k -space anisotropy⁶ have been estimated to increase its value by up to a factor of two to three as compared to the RPA result for free electrons.⁷ Indeed, a recent GW calculation⁸ confirms an enhancement of λ_0 for Cu of about a factor two; a similar value is to be expected for Au on account of its analogous electronic structure.

Soon after the invention of ballistic electron emission microscopy (BEEM), its inherent potential to deliver information about electronic transport properties was recognized, especially because of its spectroscopic capabilities (ballistic electron emission spectroscopy, BEES).^{9,10} BEEM constitutes an extension of scanning tunneling microscopy, where the tip is employed to inject hot electrons into a heterostructure composed of a metal film (typically 50–300 Å) on top of a semiconductor substrate. Electrons traveling through the metallic base layer and able to surmount the Schottky barrier at the interface are detected at a back contact as the BEEM current, rendering the technique similar to the standard procedure of using internal photoemission data for extracting electronic attenuation lengths.⁷ Nevertheless, the clear-cut energetic and spatial distribution of the locally injected hot carriers in BEES entails significant advantages over the intricate excitation by means of light radiation, and a better determination of MFP's should in principle be possible. Un-

fortunately, the basic theory underlying BEES in its first 10 years has been rudimentary, and may still be roughly described as a free-electron phase-space model, as originally proposed by Bell and Kaiser.⁹ The ensuing oversimplification of the data analysis has caused a puzzle, as independently determined MFP's were found to differ by an order of magnitude for the same metal^{11,12,14} or a functional form for $\lambda_{ee}(E)$ had to be proposed, which was in disagreement with the standard Fermi-liquid theory.¹²

A second difficulty appearing in previous attempts has been to infer error estimates exclusively from the quality of a fit to the experimental $I(V)$ -spectra, without scrutinizing the influence of physical processes that had been disregarded in the theoretical modeling. Possible cross correlations in the multiparameter fit of BEES data could induce a large uncertainty among the various MFP's for electron-electron (e-e), electron-phonon (e-p), and electron-defect (e-d) scatterings, which all contribute to the total measurable attenuation length. Obviously, it would be difficult to get from a single magnitude (e.g., the measured attenuation length) individual MFP values for the different scattering mechanisms (such as e-e, e-p, and e-d) influencing the BEEM current. Moreover, we notice that it would be unjustified to use Matthiessen's rule to combine them,¹³ as these processes can strongly interplay with each other (see, e.g., the e-p-backscattering-induced enlargement of the effective dwell time of the electron in the metal layer). Therefore, we propose to study the e-e interaction in BEES experiments by focusing on experimental conditions where other contributions can be considered negligible, i.e., low temperature and low voltages. Since there is some experimental and theoretical evidence that the e-d interaction significantly affects Au BEES data for thick films (≈ 200 – 300 Å),^{14–16} we suggest to further avoid this influence by concentrating our discussion on overlayers around ≈ 100 Å. For the model case of Au/Si(111), we show how the, then dominant, inelastic $\lambda_{ee}(E)$ can be extracted for $E > E_F$ from the experimental data, thereby finding perfect accordance with the expected Fermi-liquid theory energy dependence. Effects of elastic scatterings that are not fully accounted for in our full quantum-mechanical Green's-function (GF) description of BEES are quantitatively investigated with semiclassical k -space ensemble Monte-Carlo (MC) simulations. In this way, we obtain worst-case error bars for the retrieved magnitude of the e-e MFP.

A theoretical description of BEES has to comprise the complete current-flow scenario, which may be conveniently subdivided into four basic steps: (1) tunneling from the tip to the metal surface, (2) propagation of the hot electrons through the metallic overlayer, (3) transmission over the Schottky barrier at the metal/semiconductor contact, and (4) transport inside the semiconductor substrate. A meaningful determination of the transport parameters can only be achieved when all steps are accounted for at a considerable level of sophistication. Among the processes so far disclosed as crucial to the understanding of BEES we can cite: for step (1) the proper tunneling distribution corresponding to the electronic structure of the metallic surface; for step (2) a transport analysis conforming with the metal band structure¹⁷ and encompassing multiple reflections within the thin film;¹² for step (3) projecting and matching of the involved states at the interface together with the use of an appropriate dynamic

transmission coefficient,¹⁸ keeping in mind the possibility of non- \mathbf{k}_{\parallel} -conserving scatterings at nonepitaxial interfaces;^{19,20} finally, for step (4) phonon-induced backscattering of electrons having already overcome the barrier,²¹ while neglecting impact ionization processes¹¹ at the low energies of interest.

Taking into account all aforementioned processes, the BEES current can be written as a function of the tip voltage at $T=0$ K as

$$I(V_T) = \int_{V_0}^{V_T} dE \int_{BZ} d\mathbf{k}_{\parallel} J_{n-1,n}(\mathbf{k}_{\parallel}, E) T(\mathbf{k}_{\parallel}, E) P(E), \quad (2)$$

where the \mathbf{k}_{\parallel} integration is performed inside the first Brillouin zone of the metal²² and the energy integration covers the interval between the Schottky barrier V_0 and the applied external bias, V_T (both measured in energy units). This expression includes the four steps listed above: (1 and 2), $J_{n-1,n}(\mathbf{k}_{\parallel}, E)$ is the current arriving at the metal-semiconductor interface (atomic plane n), after being injected by the STM tip at the surface and having propagated through the metal film;¹⁷ in particular, in our calculations $I(V_T)$ is calculated for a tunneling current of 1 nA; (3), $T(\mathbf{k}_{\parallel}, E)$ is a quantum-mechanical transmission coefficient, computed by matching wave functions at the two-dimensional metal-semiconductor interface (\mathbf{k}_{\parallel} and E conservation is assumed at the interface, where the semiconductor is described within the first-Jones-zone approximation¹⁸); and (4), $P(E)$ is a dynamical factor taking into account the back scattering of electrons from the semiconductor into the metal due to interactions with phonons inside the depletion layer near the interface.

All these factors have been considered in the literature with different degrees of sophistication. Let us remark on two points central to this work: First, the importance of including band structure effects in the propagation through the metallic overlayer (steps 1 and 2). Within our GF approach $J_{n-1,n}(\mathbf{k}_{\parallel}, E)$ is given by²⁵

$$J_{ij}(\mathbf{k}_{\parallel}, E) = \frac{4e}{\hbar} \Im \text{Tr}[\hat{T}_{ij}(\mathbf{k}_{\parallel}, E) \hat{g}_{j1}^R(\mathbf{k}_{\parallel}, E) \times \hat{T}_{10} \hat{\rho}_{00}(E) \hat{T}_{01} \hat{g}_{1i}^A(\mathbf{k}_{\parallel}, E)], \quad (3)$$

which properly describes the tunneling injection through the hopping matrix \hat{T}_{01} , and the matrix density of states on the last atom of the tip $\hat{\rho}_{00}$. Furthermore, it also describes accurately the electronic transport in the metal by means of the Green's functions $g_{1i}^{R,A}$ and the hopping matrix between layers T_{ij} . In particular, we stress that the nontrivial current distributions in \mathbf{k}_{\parallel} space, which result from Eq. (3), are *essentially different* from the simple forward peaked cone assumed in free-electron propagation models.

Second, we have recently found that the e-p backscattering in the semiconductor (step 4) is more important than it was thought before. It strongly influences the determination of the inelastic MFP due to its net effect of sending back current from the semiconductor to the metal. In Eq. (2) we take this reduction into account through a factor $P(E)$ (see inset on Fig. 1, where the contribution of this scattering to the effective reflection at the interface is plotted) which is obtained from the MC simulation described below. As the

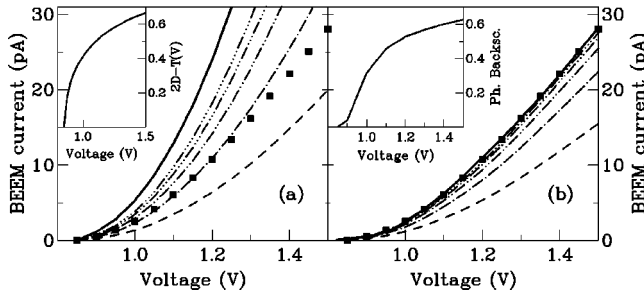


FIG. 1. $I(V)$ -curves for 75-Å Au/Si(111) at 77 K. Experimental data (solid squares in both a and b) are taken from Bell (Ref. 12). (a) Ballistic results ($\lambda_0 = \infty$) for direct injection (dashed), with one reflection at the metal surface (dashed one-dotted), with two reflections (dashed two-dotted), with three reflections (dashed three-dotted), with four reflections (dashed four-dotted), and to infinite order (solid thick line). Different reflections are calculated using the reflection coefficient obtained by matching wave functions across the (111) interface, $1 - T(E)$ [see inset in Fig. 1(a)], and the probability for an electron to be backinjected in the metal due to electron-phonon scattering in the semiconductor, $1 - P(E)$ [see inset in Fig. 1(b)]. (b) Full Green's functions result ($\lambda_0 = 16.1$ Å) decomposed in multiple reflections as in (a). The infinite order result [solid thick line in (b)] is to be compared with the experiment.

e-e interaction in the metal is the main energy-loss mechanism for the injected electrons, the backinjection combined with the e-e interaction amount to a significant reduction of the BEEM current measured at the back contact. Neglecting e-p backscattering in the semiconductor in a BEES fit would result in a shorter MFP, indicating the necessity to use a model as accurate as possible to get reliable values for the transport parameters.

With this approach, a nonparametrized description of the purely elastic BEEM current is established, which embraces all of the relevant physical processes, except for \mathbf{k}_{\parallel} violation at the interface, electron-defect scattering and nonspecular reflection at the surface, which will be addressed afterwards via the MC calculation discussed below. Moreover, a wave-field attenuation can be introduced in the GF formalism by considering a finite imaginary part of the self-energy related to the MFP in Eq. (1). This is a reasonable approach to describe the inelastic e-e interaction for $E < E_F + 1.5$ eV, since typical losses on average represent as much as half of the excess energy, $E - E_F$, ruling out subsequent transmission over the Au/Si Schottky-barrier (0.86 eV) after an e-e scattering event. Since this is the only adjustable parameter in our model, we are able to determine it accurately by a fit to experimental BEES data. Figure 1 shows our theoretical calculations and the BEES data measured by Bell for a 75-Å Au/Si(111) film at 77 K.¹² First, we display in Fig. 1(a) the results of ballistic calculations [i.e., $\lambda_0 = \infty$ and $T(E) = P(E) = 1$]. The dashed line correspond to the current injected at first attempt (i.e., no multiple reflections inside the metallic layer are considered), whereas the dashed-dotted curves show the contribution to the current of an increasing number of multiple specular reflections. In the ballistic limit an infinite number of reflections (solid thick line) means that all electrons with appropriate $(\mathbf{k}_{\parallel}, E)$ values are finally transmitted into the semiconductor. These ballistic results cannot reproduce the experimental spectrum, except

perhaps in the near-threshold region, and we are forced to introduce some kind of attenuation. Figure 1(b) shows the results of corresponding calculations where e-e interaction is considered: it is appreciated the excellent agreement between theory and experiment obtained for $\lambda_0 = 15.9$ Å (solid-thick line). As expected, for finite $\lambda(E)$ a smaller number of multiple reflections contributes to the BEEM current: we emphasize the importance of a finite e-e MFP, in spite of the fact that values of $\lambda(E)$ at lower energies are quite large compared with the actual width of the film [e.g., $\lambda(E = 1$ eV) = 574 Å]. Obviously, the difference between the ballistic model and Eq. (1) comes mainly from the region of high energies [e.g., $\lambda(E = 1.5$ eV) = 275 Å], where contributions from electrons having suffered more than four reflections at the metal surface ($L > 675$ Å) are clearly negligible for the nonballistic model. To demonstrate the accuracy of our theoretical analysis, we have found that changing by $\pm 20\%$ λ_0 produces a change in the BEEM current of less than $\pm 15\%$. Since the experimental $I(V)$ curves are likely to be determined with better accuracy, we quote a conservative error bar of $\pm 20\%$ for λ_0 . Our value $\lambda_0 = 15.9$ Å is about a factor of two larger than the standard electron gas value calculated for Au ($r_s = 3.02$, $\lambda_0^{RPA} = 9.0$ Å). Therefore, we agree, both in absolute value and in energy dependence, with theories predicting similar corrections over the electron gas value for real metals,⁸ and with values derived with different experimental techniques.^{7,26-28} Finally, it is worth mentioning that large uncertainties related to the experimental determination of inelastic e-e lifetimes abound the literature (e.g., see Table I in Ref. 1). Therefore, to get the error bars associated with our analysis it would be important in addition to estimate effects that are not contained within our GF approach: mainly diffuse reflections at the metal surface and violation of \mathbf{k}_{\parallel} conservation at the interface. To that end, we additionally performed semiclassical MC simulations in k space. This method had been successfully applied to study other important points in BEEM (e.g., the resolution degradation due to inelastic effects²³) and it will be described in detail elsewhere.²⁴ For the purpose of this work, we shall only comment on the main relevant points in the simulation: (i) as the input ensemble of electrons injected into the metal layer we use the near-surface current distribution computed by the GF method [Eq. (3)]; this is a reasonable approximation, because the MFP of the injected electrons in the Au layer is much longer than the length scale on which the current distribution reaches its asymptotic form (i.e., after four or five atomic layers); (ii) the e-e interaction is modeled by scattering rates as computed in the RPA; to be consistent with the GF calculation, we also reduce the total e-e interaction strength by a factor of 2; (iii) to estimate the influence of possible e-d scatterings, we model this interaction channel by scattering rates depending only on the assumed density of defects; (iv) to provide for the main effect of the electronic band structure on the k -space current distribution, at every stage in the simulation, a Monte-Carlo rejection technique²⁹ is applied whenever propagation inside a forbidden directional gap would happen as a result of scattering; (v) scattering of carriers at the surface is modeled by varying the relative amount of specular and diffuse reflections; (vi) non- \mathbf{k}_{\parallel} conservation at the interface is included by randomizing the current distributions over the two-dimensional (2D) Brillouin

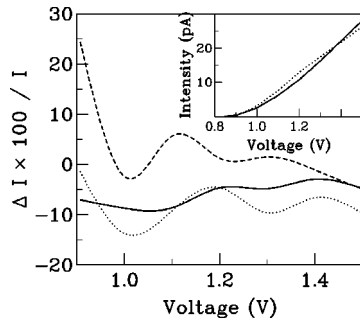


FIG. 2. A comparison between the GF (solid line) and the MC results (dotted), for the specular model and the same $\lambda_{ee}(E)$, is provided in the inset. In the figure, the relative change in intensity between the MC specular model and the three following models is given: diffuse reflections at the surface (solid line), randomization of k_{\parallel} at the interface (dotted line), and elastic scattering with defects, $\lambda_{e-d} \approx 100$ Å, (dashed line).

zone, prior to transmission over the interface; (vii) scattering of electrons with acoustic and optical phonons in the depletion layer is described via deformation potentials.²⁹ We finally remark that the number of phonon backscatterings (step vii) does not significantly depend on details of the \mathbf{k}_{\parallel} distribution of electrons entering the semiconductor, thus justifying our original inclusion of this scattering channel in Eq. (2) through a factor $P(E)$.

In the inset of Fig. 2 we compare our two approaches. For a specular-reflection model at the surface/interface and for scattering rates equal to the ones used in GF, MC is compared with the previous GF result. A fair agreement between both approaches is found. This is highly satisfactory in view of the approximations made in MC regarding the metal band structure, e.g., by performing an azimuthal average and using the initial current distribution at $E_F + 1.2$ eV for the whole energy range.²³ Next, we estimate the uncertainty in our computed BEEM current arising from effects not taken into account in our specular model by considering different scenarios in our MC simulation and by comparing with the

specular model. The solid line in Fig. 2 corresponds to the relative change in intensity when a simulation with diffuse reflection at the metal surface is performed. The dotted line represents the effect of non- \mathbf{k}_{\parallel} conserving interface scatterings,^{19,20} which is treated by allowing the pickup of an arbitrary \mathbf{k}_{\parallel} at the interface with a 40% probability. This value describes what we consider as an extreme case because in the Au/Si interface the disorder is confined to a few layers and does not affect greatly to the incident Bloch waves, suggesting that the non- \mathbf{k}_{\parallel} conserving processes are only a few percent of the total. Finally, the dashed line shows the results of a simulation with a short elastic e-d MFP of 100 Å where the differential cross section is assumed to be isotropic. From all these case studies, it is clearly observed that none of these elastic scatterings has a major influence, typically less than $\pm 10\%$, on the BEES spectra for thin metallic films. Hence, these results clearly reinforce our previous GF results and allow us to estimate a conservative worst-case error in the determined e-e MFP of $\pm 20\%$.

In conclusion, we find that an RPA-like energy dependence for the inelastic e-e MFP can account for the spectral dependence of $I(V)$ -curves measured by BEES on thin-gold metal films (on theoretical grounds, we expect this is not particular for gold). An excellent agreement between theory and experiment is achieved by increasing λ_0^{RPA} by a factor 2. These results reconcile the generally accepted theoretical ideas on electronic energy relaxation rates with recent BEES measurements. They also show the potential of BEES to investigate details of inelastic e-e lifetimes that are still under discussion. To make this complicated task more reliable it is necessary to keep the analysis of the experiments as simple as possible; in particular, we propose to perform measurements on thin samples at low temperature, with a well-characterized structure exhibiting a low concentration of defects, and to concentrate in the near-threshold region.

K.R. and K.H. are grateful for financial support from SFB292 (Germany). P.L.A., F.J.G.V., and F.F. acknowledge financial support from the Spanish CICYT under Contract Nos. PB97-28 and PB97-1224.

¹H. Petek and S. Ogawa, Prog. Surf. Sci. **56**, 239 (1997).

²J.M. Luttinger, Phys. Rev. **121**, 942 (1961).

³J.J. Quinn, Phys. Rev. **126**, 1453 (1962).

⁴J.J. Quinn, Appl. Phys. Lett. **2**, 167 (1963).

⁵R.H. Ritchie *et al.*, J. Phys. Chem. Solids **26**, 1689 (1965).

⁶S.L. Adler, Phys. Rev. **141**, 814 (1966).

⁷C.R. Crowell and S.M. Sze, in *Physics of Thin Films*, edited by G. Hass and R.F. Thun (Academic, New York, 1967), Vol. 4, p. 325ff.

⁸I. Campillo, J.M. Pitarke, A. Rubio, E. Zarate, and P.M. Echénique, Phys. Rev. Lett. **83**, 2230 (1999).

⁹W.J. Kaiser and L.D. Bell, Phys. Rev. Lett. **60**, 1406 (1988); L.D. Bell and W.J. Kaiser, *ibid.* **61**, 2368 (1988).

¹⁰M. Dähne-Prietsch, Phys. Rep. **253**, 164 (1995); L.D. Bell and W.J. Kaiser, Annu. Rev. Mater. Sci. **26**, 189 (1996).

¹¹A. Bauer *et al.*, Phys. Rev. Lett. **71**, 149 (1993).

¹²L.D. Bell, Phys. Rev. Lett. **77**, 3893 (1996).

¹³J.M. Ziman, *Electrons and Phonons* (Oxford University Press,

Oxford, 1960).

¹⁴C. Manke *et al.*, Appl. Surf. Sci. **117**, 321 (1997).

¹⁵C.A. Ventrice, Jr. *et al.*, Phys. Rev. B **53**, 3952 (1996).

¹⁶K. Reuter *et al.*, Europhys. Lett. **45**, 181 (1999).

¹⁷F.J. García-Vidal *et al.*, Phys. Rev. Lett. **76**, 807 (1996).

¹⁸P.L. de Andres *et al.*, Appl. Surf. Sci. **123**, 199 (1998).

¹⁹R. Ludeke and A. Bauer, Phys. Rev. Lett. **71**, 1760 (1993).

²⁰D.L. Smith *et al.*, Phys. Rev. Lett. **80**, 2433 (1998).

²¹E.Y. Lee and L.J. Schowalter, J. Appl. Phys. **70**, 2156 (1991).

²²R. Ramirez *et al.*, Int. J. Quantum Chem. **19**, 571 (1988).

²³U. Hohenester *et al.*, Phys. Status Solidi B **204**, 397 (1997).

²⁴U. Hohenester (unpublished).

²⁵K. Reuter *et al.*, Phys. Rev. B **58**, 14 036 (1998).

²⁶S.M. Sze *et al.*, J. Appl. Phys. **37**, 2690 (1966).

²⁷W.S. Fann *et al.*, Phys. Rev. B **46**, 13 592 (1992).

²⁸M. Aeschlimann *et al.*, Chem. Phys. **205**, 127 (1996).

²⁹C. Jacoboni and L. Reggiani, Rev. Mod. Phys. **55**, 645 (1983).